

Variations in the glass transition temperature of polyester with special architectures confined in thin films

M. Erber, A. Khalyavina, K.-J. Eichhorn*, B.I. Voit

Leibniz Institute of Polymer Research, Dresden e.V., Hohe Str. 6, D-01069 Dresden, Germany

ARTICLE INFO

Article history:

Received 6 August 2009

Received in revised form

13 November 2009

Accepted 15 November 2009

Available online 20 November 2009

Keywords:

Polymer thin films

Glass transition temperature

Confinement effects

ABSTRACT

Variations of the polymer dynamic of different systematically varied polyester architectures in the confinement of thin films were studied by temperature dependent spectroscopic *vis*-ellipsometry. The architectures were tailored in order to evaluate (a) the impact of different polymer backbones (hyper-branched, branched or linear and aromatic, aromatic–aliphatic or aliphatic), (b) the influence of functional groups (hydroxyl, benzoyl, *tert*-butyldimethylsilyl) and (c) the role of interfacial interactions (attractive, repulsive) with the silicon substrate. Possible reasons for the deviation of the glass transition temperature T_g in thin polymer films (10–800 nm) from the bulk value are described and compared to the literature. It was found that the functional groups of the applied polymers have the largest effect on T_g . Beside interfacial interactions, chemical and physical reactions in the polymer film are playing a significant role.

© 2009 Elsevier Ltd. All rights reserved.

1. Introduction

The manipulation and characterization of materials on the micro- or nanoscale contribute more and more to modern material science and new developments in industry. Especially polymers in thin films have very important applications in the field of coating, protection and fine-tuning of surface properties, as well as in microsystems and microelectronic devices e.g. as materials for soft lithography, photoresists, disk drive lubricants, chemical sensors and so on. Although the physics of bulk polymers has been analyzed extensively, the properties of thin polymer films and surfaces are still rather poorly understood and confront scientists with severe problems [1–6].

One of the current challenges is to determine how the T_g and thus the dynamics in thin polymer films may differ from bulk material. In general, with decreasing film thickness the surface to volume ratio increases dramatically and hence interfacial interactions are expected to dominate the molecular dynamic of geometrical confined polymers. But even though this has been studied extensively and is the topic of comprehensive reviews [1–5], no consistent picture has yet been determined. In some cases where interfacial forces are attractive they can inhibit cooperative dynamics and lead to a rise in T_g [1,7–9]. On the other hand, polymer chains can show increased dynamics, e.g. shift of T_g to

lower values, if repulsive or rather weak interfacial interactions are present [8–12]. A vast number of experimental tools (X-ray/Neutron Reflectometry [13,14], Dielectric Spectroscopy [15–17], AC-Calorimetry [18], Ellipsometry [4,7,19–22] etc.) measuring microscopic or macroscopic physical quantities are applied to investigate the T_g behaviour in confined geometry. In most cases well-known simple linear homopolymers like poly(methyl methacrylate) (PMMA) or polystyrene (PS) are investigated as model systems. However, other polymer architectures like dendritic macromolecules are likely to exhibit much different properties than their linear counterparts due to the highly branched structure and high number of functional groups [23]. Developed on the idea of simplifying the complicated, time-consuming and therefore cost intensive step-wise synthesis of dendrimers without losing their dendritic character, hyper-branched (hb) polymers are of special interest. Unlike the perfect structure of dendrimers with a degree of branching of about 100% hb polymers possess only a less perfect three dimensional molecular structures with a statistical degree of branching of 50% including linear, dendritic and terminal units. However, these polymers show many of the properties of dendrimers; globular structure, similar viscosity behaviour attributable to significantly reduced entanglements and multitude end-groups. Serghei et al. were the first who investigated thin films of hb aromatic polyesters using capacitive scanning dilatometry and broadband dielectric spectroscopy [17]. Depending on the experimental techniques, a divergence of T_g as a function of film thickness $T_g(d)$ was reported. An increase of about ~ 10 K determined by means

* Corresponding author. Tel.: +49 351 4658 256; fax: +49 351 4658 362.
E-mail address: kjeich@ipfdd.de (K.-J. Eichhorn).

of capacitive scanning dilatometry was observed for the thinnest film (17 nm) analyzed while the temperature position of the alpha relaxation peak was shifted by ~ 30 K to lower temperatures. Remarkably, these deviations from bulk T_g with decreasing thickness start already at unusual high thickness value of about 200 nm. This communication shows the need of more experimental and analytical work for a better understanding of these extraordinary architectures in confined geometry.

Inspired from that we report detailed investigations on T_g in thin films of newly synthesized hb polyester architectures as well as their linear counterparts. The polyesters were chemically tailored in order to determine the role of the polymer architecture on T_g in thin films down to 10 nm.

2. Materials and methods

2.1. Materials

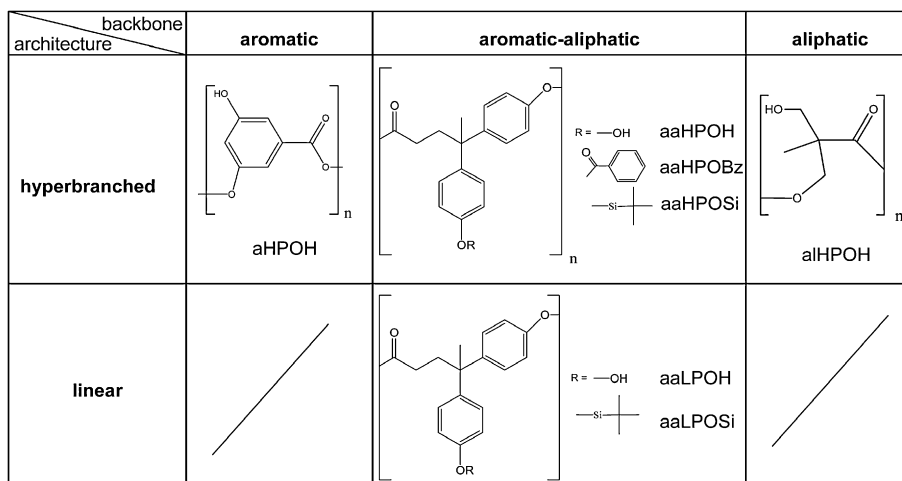
Hyperbranched hydroxyl terminated polyesters with a fully *aromatic* (aHPOH) or *aliphatic* (alHPOH) backbone were synthesized in melt using suitable AB_2 monomers (Scheme 1) [23]. The **hb aromatic–aliphatic** polyester with hydroxyl groups (aaHPOH) was synthesized in solution at mild conditions according to a recently published article of our group (Scheme 2) [24]. The quantitative modification of the end-groups was carried out with benzoyl chloride and *tert*-butyldimethylsilyl chloride, respectively [24–26]. For reasons of comparability, the **linear aromatic–aliphatic** polyesters (aaLPOSi, aaLPOH) were synthesized from the same AB_2 monomer as applied for the hb analogue [26]. To prevent branching one functional OH group in the monomer was chemically capped and than in a further step polymerized to obtain aaLPOSi [26]. For a fully OH terminated linear polyester (aaLPOH), the protecting groups (*tert*-butyldimethylsilyl (TBDMS)) from aaLPOSi were cleaved via mild acidic hydrolysis [26]. During the cleavage, the degradation of the polymer backbone was not avoidable yielding a much lower molecular weight polymer (Table 1). The structure of all polymers was proved by extensive SEC, NMR- and IR spectroscopy measurements. Thermal properties of the bulk materials were characterized by TGA and DSC. Unless otherwise stated, all substances and solvents were purchased with the highest purity grade from commercial sources (Sigma–Aldrich, Fluka or Acros) and inserted as received.

2.2. Film preparation

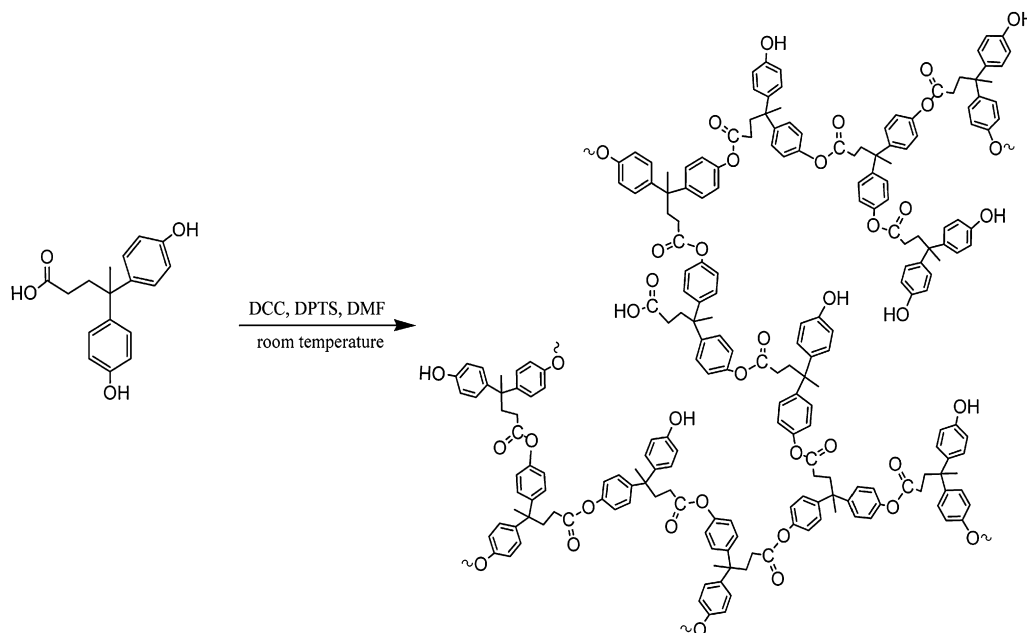
Silicon wafers with a native silicon dioxide layer (~ 2 nm) were used as substrates. Dust particles and organic contaminations were removed in an ultrasonic bath first in dichloromethane and afterwards in acetone. In an additional step, the substrates were placed in an alkaline hydroperoxide solution mixture (Milipore® water (18 M Ω cm), hydrogen peroxide (30%) and ammonia solution (25%), in the volume ratio 5:1:0.5) for 20 min resulting in hydrophilic surfaces (static water contact angle below 5°). The substrates were carefully rinsed in Milipore® water and directly used. The root-mean-square roughness (rms) of the purified silicon surface was below 0.3 nm measured by means of AFM. All films were prepared by spin-coating at moderate spinning speed (3000 rpm) and spinning time (30 s) from different concentrated solutions (methyl ethyl ketone for aHPOH and aaHPOSi, 4-methyl-2-pentanone for aaHPOH and aaLPOH, toluene for aaHPOBz, ethanol for alHPOH). Afterwards, the films were annealed in the ellipsometer heat cell under defined atmosphere (Ar) for at least 15 h well above T_g and boiling point of the applied solvent in order to obtain a fully equilibrated polymer film. The quality of all applied polymer films was checked by optical microscopy and AFM before and after annealing to exclude dewetting (Fig. 1).

2.3. Ellipsometric measurements

In general ellipsometry measures a change in polarization as polarized light reflects from a bare surface or thin film. The polarization change is represented as amplitude ratio ($\tan\Psi$) and phase difference (Δ). The measured response is dependent on optical properties (refractive index n , extinction coefficient) and the thickness d of each film. Further details on ellipsometric fundamentals are given in the Refs. [28,29]. Our temperature dependent spectroscopic ellipsometry measurements were carried out at a fixed angle of incidence (70°) using a multi wavelength (370–1680 nm) rotating compensator ellipsometer (RCE) M2000VI (J. A. Woollam Co., Inc., USA) connected with a heat cell (INSTEC Inc., USA). The real temperature on the surface of a silicon wafer during heating/cooling was checked in a separate calibration experiment by different melt transition standards from Perkin Elmer (Sn, Pb, In, Zn) commonly used for calorimetry. The standards were melted to the wafer surface at appropriate temperature, then cooled, and reheated to record the melt transition and corresponding



Scheme 1. Simplified chemical structure of the investigated polymers.



Scheme 2. Synthetic approach for aaHPOH under mild conditions.

thermometer reading. By visually observing the consecutive melting points for the standards at a ramp of 2 K/min, the temperature was checked within an accuracy of ± 1 K in the applied temperature range (25–420 °C). Recording of the ellipsometric data and heating/cooling were coordinated and controlled by the software (Complete Ease, J. A. Woollam Co., Inc. USA) [30]. Measurements were performed under argon flow at a moderate scanning rate of 2 K/min. The layer thickness d and the refractive index n were fitted to the ellipsometric angles Ψ and Δ measured in the entire wavelength range assuming the layer stack Si/SiO₂/polymer/ambient as optical model. The extinction coefficient k of all polyesters was checked to be zero in the used wavelength range. Values for the optical constants of the applied substrates (Si, SiO₂) were taken from the literature [29]. A Cauchy dispersion for the wavelength dependence of the polymer refractive index n was assumed. It should be noted that changes in the optical properties of the substrate (Si) with temperature can have significant impact on the thickness accuracy of thin films [19]. Therefore, temperature dependent data from the software (Complete Ease) [28] were used in which the optical properties of Si are stored as a function of temperature.

Table 1
Selected properties of the synthesized polyesters.

Sample	Functional groups	M_w [g/mol] ^a	M_w/M_n ^a	DB [%] ^b	T_{dec} ^c	T_g^d
aHPOH	–OH	27,200	3.2	60%	330 °C	218 °C
aaHPOH	–OH	14,800	9.8	50%	270 °C	119 °C
aaHPOBz	–benzoyl	37,200	4.5	50%	275 °C	115 °C
aaHPOSi	–TBDMS	24,200	2.8	50%	301 °C	97 °C
aaLPOH	–OH	6500	2.1	0%	235 °C	110 °C
aaLPOSi	–TBDMS	64,000	3.3	0%	295 °C	115 °C
alHPOH	–OH	21,700	6.4	45%	219 °C	34 °C

^a Determined via SEC coupled to differential refractive index (RI) detector and multi angle laser light scattering-detector (MALLS). In order to achieve complete information about the molar mass distribution of the samples, fitting of the molar mass/elution volume dependence for the whole elution region covered by RI-signal has been applied. The dn/dc was determined by estimating 100% mass recovery.

^b Degree of branching according to Frey's formula [27].

^c Onset of the polymer main decomposition determined with TGA under nitrogen flow at 10 K/min.

^d Bulk T_g determined by means of DSC at 2 K/min using the half-step method.

The T_g of a thin polymer film can be determined using the ellipsometric data in a variety of ways but always the discontinuity (“kink”) in the thermal expansion was detected as function of film thickness during heating at constant rate and defined as T_g . Firstly by using the “raw data” (Ψ and Δ), hence T_g can be determined from the discontinuity in Ψ and/or Δ curves (plotted for a particular wavelength) as a function of temperature (Fig. 2) [7]. Furthermore, the full spectroscopic data set of Ψ and Δ can be also fit with an appropriate optical model to yield the thickness and refractive index of the polymer film as a function of the temperature [2,4]. The discontinuity in either d or n as a function of temperature can be used to determine T_g (Fig. 4). However, the temperature dependence of n and d instead of individual Ψ and Δ is more appropriate for several reasons. Ψ and Δ have to be measured at a fixed and most sensitive wavelength that has to be determined from a wide range of wavelengths in an additional step. Certainly, measurements on one wavelength increase the probability of getting noisy curves due to a less sensitive wavelength. Additional information

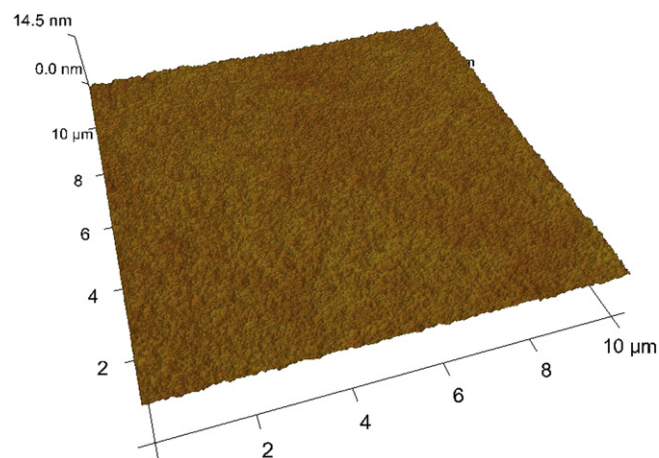


Fig. 1. Representative AFM picture of a 100 μm^2 capture after sufficient annealing. The root-mean-square roughness (rms) is below 0.5 nm.

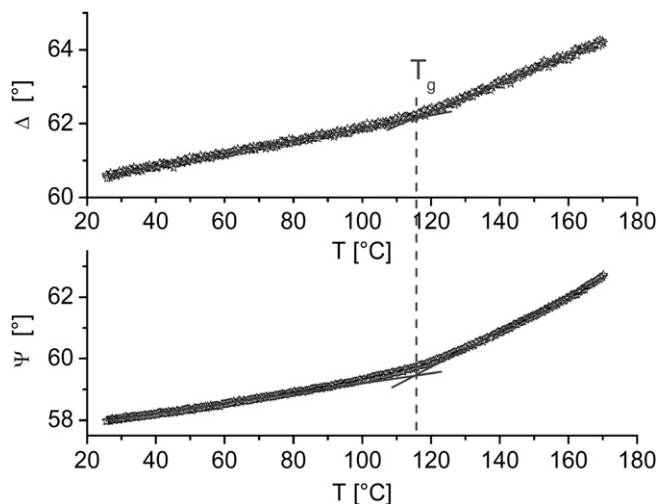


Fig. 2. Ellipsometric “raw data” (Ψ and Δ) at a sensitive wavelength ($\lambda = 589$ nm) as a function of temperature for a representative polymer film on SiO_2 with an initial thickness of about 100 nm. The dashed line serves as guidance for the eyes.

can be derived from the temperature dependence of n and d (for instance coefficient of thermal expansion, mass-loss) [19]. To find the exact T_g , we calculated the second derivatives of $d(T)$ and $n(T)$ and used the maximum and minimum values of the resulting curves, respectively (Fig. 3). All of these data analysis methods can be applied to determine T_g and it was generally found that the methods yielded T_g values that were in good agreement for thicker films ($d > 50$ nm). Especially the T_g determination via the second derivative is a convenient and accurate method in very thin polymer films. Therefore, the T_g results reported in this paper are determined in this manner. T_g measurements obtained in several heating and cooling cycles being consistently within ± 2 K or less.

At this point it is worth to note, that with decreasing length scale the contrast of the glass transition defined as the ratio of the rubber expansivity α_{rubber} to that of the glass α_{glass} is decreasing for very thin films [2]. As the contrast of the transition decreases, it becomes more and more difficult to identify the transition and is by definition not possible for a contrast value of 1.

$$\text{contrast} = \frac{\alpha_{\text{rubber}}}{\alpha_{\text{glass}}} \geq 1 \quad (1)$$

In practice, any data exhibit scatter and noise, and the identification of T_g becomes impossible for very thin films. In our measurements with film thicknesses ~ 20 nm the overall changes

in ellipsometric angles with increasing temperature are so small that the difference in slope above and below T_g is obscured by the noise level in the data. Furthermore, slight non-linearity in the dependence of ellipsometric angles on film thickness are particularly problematic as well as the separate determination of n and d due to parameter correlation for very thin films. Therefore, for films with a thickness below 20 nm the refractive index was fixed to n_{bulk} calculated for thick films ($d > 100$ nm) using a Cauchy dispersion. With this approach the thinnest films (~ 10 nm) were analyzable with good accuracy. Below 10 nm the noise of the data was just adequate but the changes in thickness and refractive index are very small and hence the determination of T_g is afflicted with a distinctive experimental error up to ± 10 K. Such difficulties lead to an effective lower limit of sensitivity in our technique to determine T_g in extremely thin films and therefore such films are not used in this report.

2.4. Modelling

A number of different mechanisms and models have been proposed to describe T_g in the confined geometry of a thin film [1–6]. To the best of our knowledge, no fundamental model is successfully able to accurately capture all of the observed experimental phenomena and therefore all models are still controversially discussed. However, our data can be fit, in principle, using Eq. (2) reported by Kim et al. [31]

$$T_g(d) = T_{g,\text{bulk}} \left[\frac{d(2k+d)}{(\xi+d)^2} \right] \quad (2)$$

This relation is based on the continuous multilayer model (CMM) which assumes that the polymer film is divided into an infinite number of sublayers, where each of them has a different glass transition temperature. The CMM air–polymer surface was characterized by a lower T_g than the bulk, while close to the substrate a higher T_g was assumed due to polymer/substrate attractive interactions. The CMM then provides an explicit expression for $T_g(d)$ expected for a certain film thickness d , where k and ξ are two adjustable length-scale parameters that account for the substrate–polymer and air–polymer interactions, respectively. The CMM is contradictory to a number of other empirical models that only describe a monotonic decrease in $T_g(d)$ because attractive substrate interactions are not taken into account [2]. The CMM model was used to fit the experimental results for all applied polyester systems sufficient accurate to fit the experimental results for all applied polyester systems but depending on the more or less

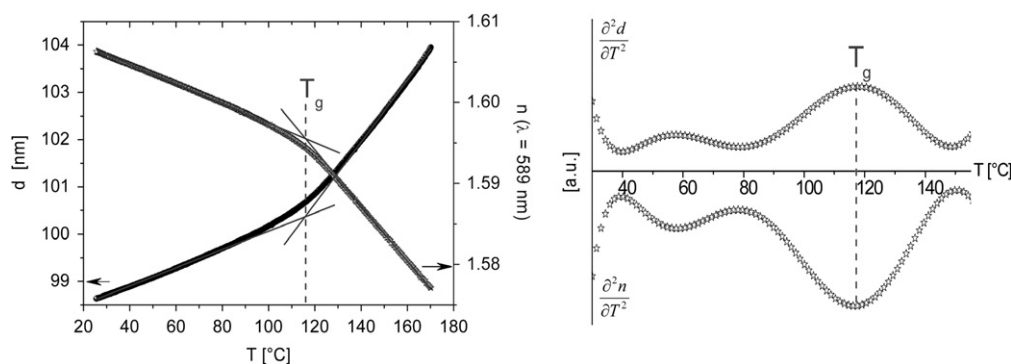


Fig. 3. Dynamic n (refractive index) and d (film thickness) scan of an aaHPOBz film on SiO_x (left) and corresponding second derivative of $d(T)$ and $n(T)$ (right). The dashed line serves as guidance for the eyes.

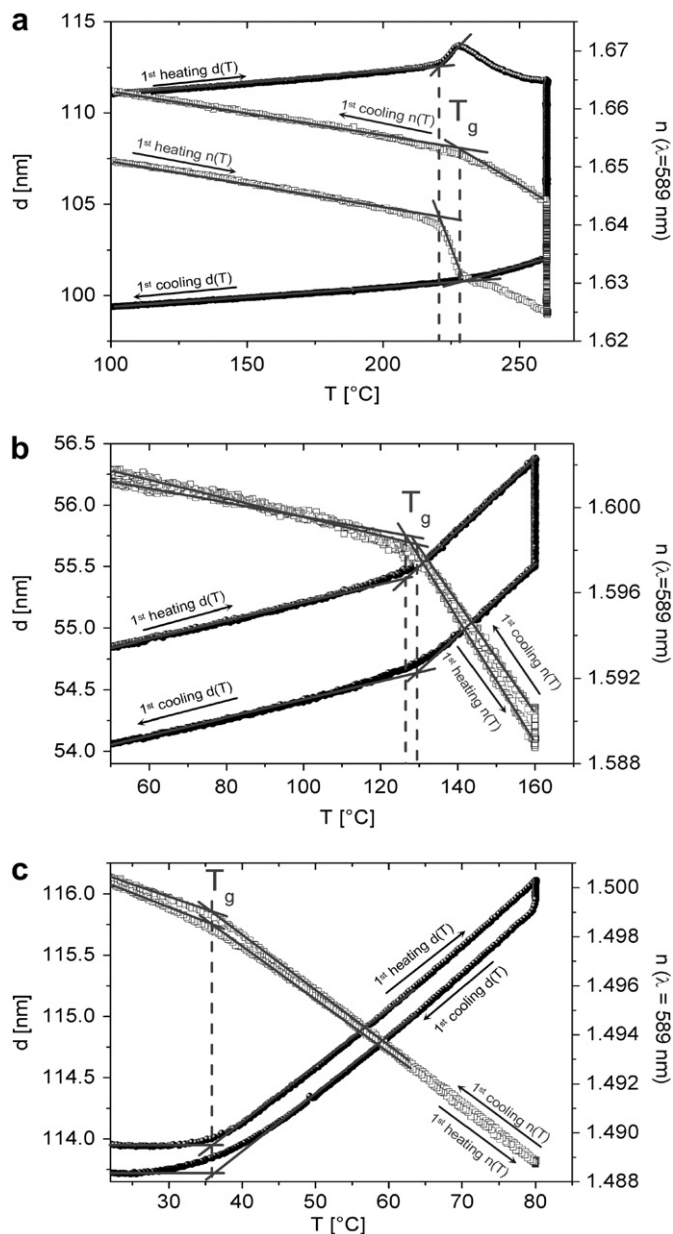


Fig. 4. Dynamic scan of film thickness d (filled circles) and refractive index n (open squares) with an additional isothermal period at appropriate temperature for at least 15 h for different “reactive” OH terminated hb polyester on SiO_x : (a) aHPOH (b) aaHPOH and (c) alHPOH.

pronounced curve trend the deduced parameter k and ξ are afflicted with a large fit error.

3. Results and discussion

3.1. Hydroxyl terminated polyester

As mentioned in the Introduction, Serghei et al. [17] have primarily investigated a hb aromatic polyester with both hydroxyl and acetyl groups. For our studies we synthesized a fully hydroxyl terminated hb aromatic polyester similar to the one described in the previous paper [17] but with a significant higher amount of OH groups (Table 1). Hence, increased attractive interactions via hydrogen bonds are assumed. As widely described in literature, annealing is done well above T_g and the boiling point of the applied

solvent to obtain fully equilibrated polymer films [16]. Due to the high bulk T_g (218 °C) of the polyester, annealing was performed at appropriate higher temperature (260 °C) under inert gas atmosphere (Ar) to prevent oxidation. According to TGA analysis the bulk polymer degradation starts beyond 330 °C, significantly higher than the applied annealing temperature. However, heating the film to 260 °C shows clearly that the film starts to densify and exceed the thermal expansion (Fig. 4a). After the heat treatment the film is no longer soluble in the solvent used for spin-coating, and T_g increases ($\Delta T_g = 9$ K) which points to the formation of chemical and physical networks [32,33]. As reported in the article from Reichelt et al. on similar OH terminated hb polyesters such thermal induced reactions are ascribed to inter- and intra-molecular chemical and physical reactions [32]. These reactions proceed in two steps: (a) the polyester is anchored to the silicon substrate via hydrogen bonds and via covalent bonds between the hydroxyl groups in the polymer and the silanol groups on the silicon surface, (b) after long annealing times transesterification and ether groups are formed between available hydroxyl groups. However, detecting such side reactions are very demanding due to the very low concentration in the polymer.

To prevent such thermally induced chemical reactions another hb polymer system (aaHPOH) with a lower bulk T_g (118 °C) was synthesized. Again, the samples were annealed well above T_g (160 °C) (Fig. 4b). Surprisingly, here the same feature as found for aHPOH was detected. Even after long annealing time also at lower temperatures, no equilibrium conformation was found and again the polymer films were no longer soluble after heat treatment. In order to have the identical thermal history a series of aaHPOH were heat-treated under the same conditions (1 h at 160 °C; T_g determined from 1st cooling scan). A significant rise in T_g (14 K) with decreasing film thickness was found for the thinnest film of aaHPOH that could be analyzed (70 nm) (Fig. 5, upper curve). We assume that a small heat gradient (from the bottom to the top of the polyester film) in the heat cell is omnipresent and induce chemical and/or physical crosslinking. Therefore, for thinner films it is possible that the percentage amount of crosslinks is higher than for thicker films leading to higher T_g values. Beside the network formation it is of course possible that manifold attractive interactions (inter- and intra-molecular H bonds) influence T_g in confined geometry.

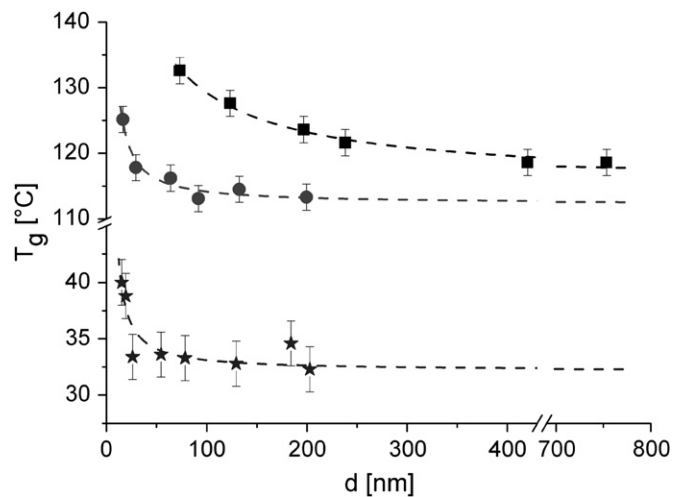


Fig. 5. T_g as a function of film thickness d for different “reactive” polyester on SiO_x : stars = alHPOH, circles aaLPOH and squares = aaHPOH. The dashed lines correspond to the fit of the experimental data using Eq. (2).

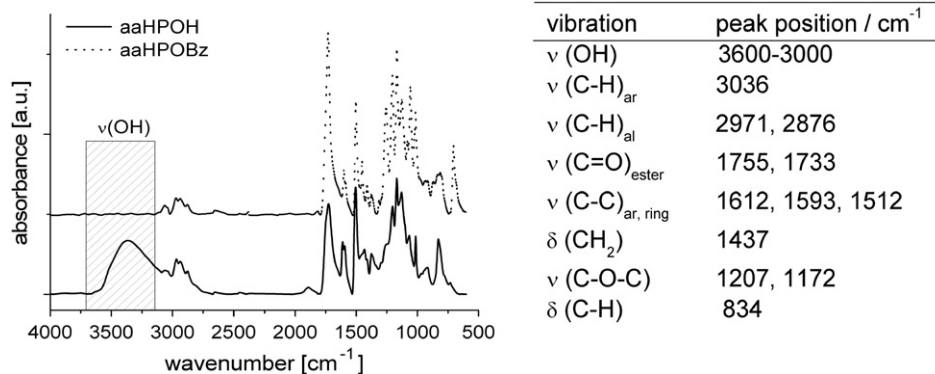


Fig. 6. FTIR-spectra of OH terminated aaHPOH as well as of the fully capped aaHPOBz (left), corresponding band assignment (right).

To determine the role of polymer architecture on T_g , a linear aromatic–aliphatic polyester (aaLPOH) was investigated which is synthesized from the same AB₂ monomer as used for the hyper-branched aaHPOH and therefore has also a functional group in each repeating unit. The films were annealed for several hours well above the T_g and again densification occurred during annealing at 160 °C (for 14 h, $\Delta d = 4.5$ nm) together with a rise in T_g ($\Delta T_g = 6$ K). Nevertheless, T_g as a function of film thickness was determined under comparable experimental conditions (Fig. 5). Similar to aaHPOH T_g increases (~ 11 K) with decreasing film thickness due to the formation of networks as well as manifold attractive interactions.

So, we can conclude that all hydroxyl terminated aromatic and aromatic–aliphatic polyesters in confined geometry are quite sensitive to higher temperatures (>160 °C) with the change of crosslinking or build-up of strong physical networks and therefore, absolute care must be taken if such polar and reactive polymers in thin films are under thermoanalytic investigation.

As a thermally stable alternative an aliphatic hb polyester (alHPOH) with a significant lower bulk T_g (~ 34 °C) was tested. Again, all films were annealed but in that case 80 °C were sufficient (Fig. 4c). All annealed alHPOH films were, in contrast to the other HPOH, completely soluble in the appropriate solvent after thermal treatment and hence nearly no densification took place and no network was formed after annealing. Nevertheless, T_g is shifted again to higher temperatures (~ 8 K) for films below 25 nm (Fig. 5). The reason for that feature cannot be crosslinking but rather

manifold attractive interactions via inter- and intra-molecular H bonds.

3.2. Chemically capped polyester

To prevent thermally induced reactions in hb aromatic–aliphatic polyester system (aaHPOH) all reactive OH groups were chemically capped using benzoyl chloride [25]. According to ¹H NMR and FT-IR spectroscopy quantitative modification was observed (Fig. 6). Upon annealing at 160 °C for 19 h in argon atmosphere only a moderate decrease in film thickness ($\Delta d = 0.3$ nm) was found for aaHPOBz (Fig. 7). By monitoring n and d for a pure silicon wafer under the same annealing conditions a thermal drift of the setup in the same order of magnitude was determined. So we can conclude that aaHPOBz is thermostable in the desired heat region, which means no chemical changes take place, and hence reproducible results can be obtained. As can be clearly seen in Fig. 8, no significant deviations from bulk T_g could be determined for aaHPOBz in the thickness range of 340–12 nm within the experimental error of ± 2 K. From Ellison et al. it is known that for polystyrene thin films different modifications of the PS repeating unit structure largely influence the confined T_g [34]. For instance a dramatic T_g reduction for a 25 nm thin poly(4-*tert*-butylstyrene) film of about 47 K relative to the bulk T_g was analyzed. There, beside

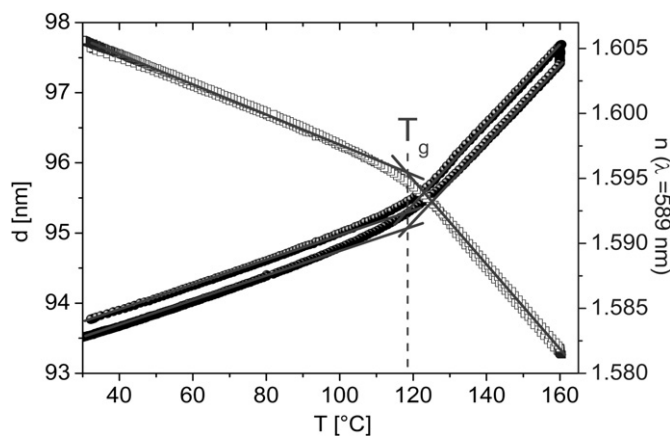


Fig. 7. Dynamic scan of film thickness d (filled circles) and refractive index n (open squares) for aaHPOBz on SiO_x with an additional isothermal period at 160 °C for 19 h. Only a simulated, marginal densification ($\Delta d = 0.3$ nm) is found due to a thermal drift in the setup.

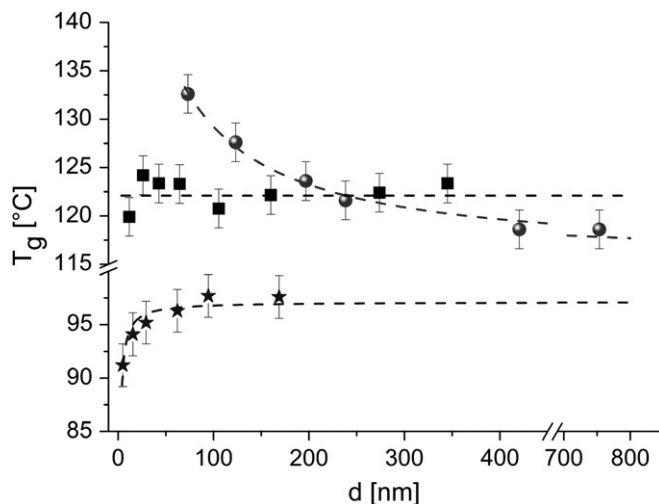


Fig. 8. T_g as function of film thickness for different hb aromatic–aliphatic polyester on SiO_x (stars = aaHPOSi, squares = aaHPOBz, circles = aaHPOH). The dashed line corresponds to the fit of the experimental data using Eq. (2).

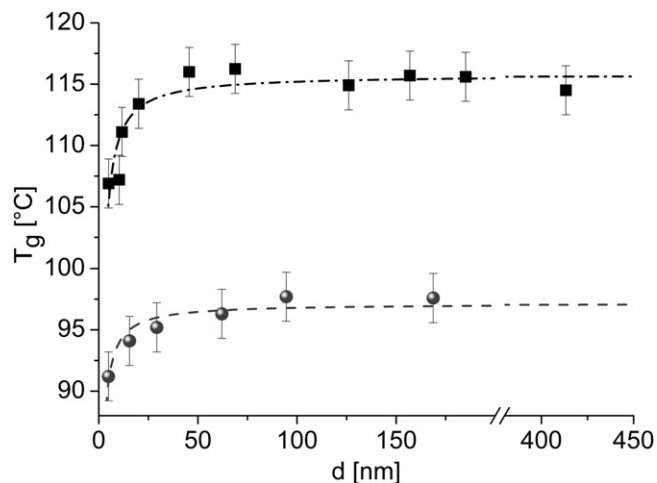


Fig. 9. T_g as function of film thickness for aaHPOSi (circles) and aaLPOSi (squares). The dashed line corresponds to the fit of the experimental data using Eq. (2).

benzoyl chloride, also *tert*-butyldimethylsilyl chloride was used to quantitatively modify aaHPOH to yield aaHPOSi [26]. Remarkably, a T_g depression of about 6 K was found for the thinnest aaHPOSi film analyzed (Fig. 8). We assume that in the case of aaHPOBz attractive and repulsive interfacial interactions are just balanced whereas for aaHPOSi stronger repulsive interactions lead to a considerable decrease in T_g . The water contact angle of aaHPOSi (96°) increases by about 14° and 19° , respectively, in comparison to the benzoyl terminated polyester (82°) and to the fully OH terminated polyester (77°). This feature clearly shows, that small modifications on the functional groups may change the interfacial interactions and therefore, the T_g behaviour of polymer films in confined geometry.

Finally, we modified similar to aaHPOSi all hydroxyl groups of a linear aromatic-aliphatic polyester (aaLPOH) to form aaLPOSi [25]. After several hours at appropriate temperature an equilibrium conformation of the polymer film was observed and crosslinking was avoidable. Similar to the hyperbranched aaHPOSi, the linear aaLPOSi shows a depressed T_g (9 K) for the thinnest films analyzed (Fig. 9). An explanation for the slightly more pronounced T_g behaviour of aaLPOSi in comparison to aaHPOSi could be the fact that aaLPOSi exhibits a much higher molecular weight and hence a much higher amount of functional groups per molecule define the interactions. Nevertheless it can be concluded that a T_g depression takes place independent of the molecular architecture (hb or linear) if the same type of functional groups is present.

4. Conclusion

We have shown for different hb polyesters as well as for their linear counterparts that T_g in confined geometry may increase or decrease, depending of the nature of the functional end or side groups. For fully OH functionalized polyesters a significantly increased T_g (max. 14 K) was found in confined geometry. However, when the annealing temperature was higher than $\sim 130^\circ\text{C}$ chemical and physical crosslinks vitrify the polymer film and hence T_g was shifted to higher values. But also below this temperature, as for alHPOH (annealing at 80°C), an increased T_g of about 8 K was determined in confined geometry due to manifold inter- and intra-

molecular H bonds. Furthermore, different protecting groups were incorporated into the polyester backbone in order to prevent crosslinking and to evaluate the influence of such groups on T_g . Remarkably, a significantly depressed T_g (9 K) could be found using *tert*-butyldimethylsilyl as functional groups due to strong repulsive interfacial interactions whereas for benzoyl groups interfacial interactions are well balanced and hence no significant deviations of T_g in bulk and confined geometry were found.

A significant result of this study is that independent of the molecular architecture (hyperbranched or linear) of the functional polymers the same T_g behaviour in thin films was found. Therefore, it is obvious, that the dynamics in confined geometry is governed by physical and chemical interactions between the substrate and the functional units as well as among the polymers.

Acknowledgement

The authors acknowledge for financial support for this study by DFG (EI 317/4-1). Furthermore we thank F. Kremer and A. Serghei (Leipzig University) for fruitful discussion and our colleagues at the IPF namely U. Georgi, S. Boye, E. Schierz, and R. Schulze, for their manifold help and support.

References

- [1] McKenna GB. *Eur Phys J Spec Top* 2007;141:291–301.
- [2] Roth CB, Dutcher JR. *J Electroanal Chem* 2005;584:13–22.
- [3] Grohens Y, Hamon L, Reiter G, Soldera A, Holl Y. *Eur Phys J E* 2002;8:217–24.
- [4] Forrest JA, Dalnoki-Veress K. *Adv Colloid Interface Sci* 2001;94:167–96.
- [5] Alcoutlabi M, McKenna GB. *J Phys Condens Matter* 2005;17:R461–524.
- [6] Sharp JS, Teichroeb JH, Forrest JA. *Eur Phys J E* 2004;15:473–87.
- [7] Keddie JL, Jones RAL, Cory RA. *Faraday Discuss* 1994:219–30.
- [8] Grohens Y, Papaleo RM, Hamon L. *Eur Phys J E* 2003;12:S81–5.
- [9] Fryer DS, Nealey PF, de Pablo JJ. *Macromolecules* 2000;33:6439–47.
- [10] Keddie JL, Jones RAL. *Isr J Chem* 1995;35:21–6.
- [11] Priestley RD, Broadbelt LJ, Torkelson JM, Fukao K. *Phys Rev E* 2007;75.
- [12] Kawana S, Jones RAL. *Phys Rev E* 2001;6302.
- [13] Wallace WE, Vanzanten JH, Wu WL. *Phys Rev E* 1995;52:R3329–32.
- [14] Miyazaki T, Inoue R, Nishida K, Kanaya T. *Eur Phys J* 2007;141:203–6.
- [15] Fukao K, Koizumi H. *Phys Rev E* 2008;77.
- [16] Serghei A. *Macromol Chem Phys* 2008;209:1415–23.
- [17] Serghei A, Mikhailova Y, Eichhorn K-J, Voit B, Kremer F. *J Polym Sci Part B Polym Phys* 2006;44:3006–10.
- [18] Huth H, Minakov AA, Serghei A, Kremer F, Schick C. *Eur Phys J Spec Top* 2007;141:153–60.
- [19] Kahle O, Wielsch U, Metzner H, Bauer J, Uhlig C, Zawatzki C. *Thin Solid Films* 1998;313:803–7.
- [20] Dalnoki-Veress K, Forrest JA, Murray C, Gigault C, Dutcher JR. *Phys Rev E* 2001;6303.
- [21] Campoy-Quiles M, Sims M, Etchegoin PG, Bradley DDC. *Macromolecules* 2006;39:7673–80.
- [22] Erber M, Eichhorn K-J, Voit B. *Polym Mater Sci Eng* 2008;99:69.
- [23] Voit BI. *C. R. Chim.* 2003;6:821–32.
- [24] Schallausky F, Erber M, Komber H, Lederer A. *Macromol Chem Phys* 2008;209:2331–8.
- [25] Reichelt S, Eichhorn K-J, Aulich D, Hinrichs K, Jain N, Appelhans A D, et al. *Colloids Surf B* 2009;69:169–77.
- [26] Khalyavina, A., Lederer, A., in press.
- [27] Holter D, Burgath A, Frey H. *Acta Polym* 1997;48:30–5.
- [28] Guide to using WVASE32, Spectroscopic Ellipsometry Data Acquisition and Analysis; J.A. Woollam Co., Inc.
- [29] Complete EASE™ software manual version 3.18. J.A. Woollam Co., Inc.; 2007.
- [30] Azzam RMA, Bashara NM. *Ellipsometry and polarized light*. Amsterdam: North Holland Publishing Company; 1977.
- [31] Kim JH, Jang J, Zin WC. *Langmuir* 2000;16:4064–7.
- [32] Reichelt S, Gohs U, Simon F, Fleischmann S, Eichhorn K-J, Voit B. *Langmuir* 2008;24:9392–400.
- [33] Mikhailova Y, Adam G, Haussler L, Eichhorn K-J, Voit B. *J Mol Struct* 2006;788:80–8.
- [34] Ellison CJ, Mundra MK, Torkelson JM. *Macromolecules* 2005;38:1767–78.